JACS
JOURNAL OF THE AMERICAN CHEMICAL SOCIETY
Article
pubs.acs.org/JACS

Redox-Modulated Stepwise Photochromism in a Ruthenium Complex with Dual Dithienylethene-Acetylides

Bin Li,[†] Jin-Yun Wang,[†] Hui-Min Wen,[†] Lin-Xi Shi,[†] and Zhong-Ning Chen*[,†,‡]

[†]State Key Laboratory of Structural Chemistry, Fujian Institute of Research on the Structure of Matter, Chinese Academy of Sciences, Fuzhou, Fujian 350002, China

[‡]State Key Laboratory of Organometallic Chemistry, Shanghai Institute of Organic Chemistry, Chinese Academy of Sciences, Shanghai 200032, China

Supporting Information

ABSTRACT: Achieving stepwise photochromism in a combined molecule to access all of the possible ring-open/closed isomers is a challenge due to facile energy transfer from ring-open dithienylethene (DTE) to an adjacent ring-closed moiety that prohibits further photocyclization. The preparation, characterization, and photochromic properties of a bis(σ-acetylide) bonded ruthenium(II) complex **2oo** and its oxidized form **2oo**$^+$ with two identical DTE-acetylides (L1o) are described. Stepwise and dual photochromic reactions are successfully achieved in both **2oo** and **2oo**$^+$, in which the ring-closing absorption band of **2oo**$^+$ shows an obvious blue-shift relative to **2oo**. It is demonstrated that stepwise photochromic reactions **2oo**→**2co**→**2cc** are more facile than **2oo**$^+$→**2co**$^+$→**2cc**$^+$. The lower electronic density at the reactive carbon atoms upon oxidation of Ru(II) to Ru(III) causes photocyclization to have more difficulty proceeding in oxidized species **2oo**$^+$/**2co**$^+$. Upon dual ring-closure, **2cc**/**2cc**$^+$ exhibits significant electronic interaction between two identical ring-closed DTE units across *trans*-Ru(dppe)$_2$ spacer. The interconversion processes among six states are unambiguously demonstrated by NMR, UV−vis−NIR, and IR spectroscopic, and electrochemical and computational studies.

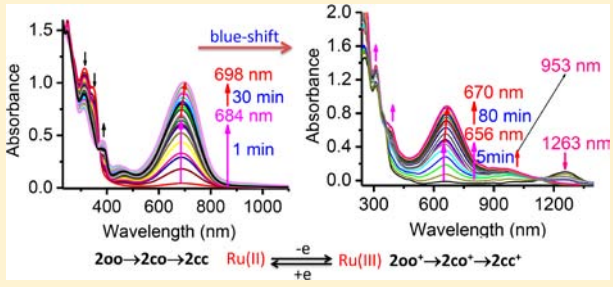

INTRODUCTION

Photochromic dithienylethene (DTE) compounds that can undergo a reversible switch between two isomers upon irradiation with appropriate light have been intensively investigated due to their extensive applications in optical memory, optoelectronics, and switching devices at the molecular level.[1−9] Recently, the combined systems composed of two or more photochromic switches are of particular interest as they can display multicolors and multistates upon irradiation with appropriate wavelengths of light,[10,11] which are particularly significant for achieving multifrequency optical memories and data storage.

When two or more DTE moieties in a combined molecule are totally separated by nonconjugated organic or organometallic spacers, they always operate independently without direct interaction between them. Each DTE unit behaves as an isolated switching system so that ring-closure occurs simultaneously at several identical DTE moieties to afford the fully ring-closed form.[11−16] Low-energy absorbance due to ring-closing reaction is simply accumulation of several independent DTEs without changes or shifts in wavelengths. In this case, stepwise ring-closed products containing both ring-open and -closed DTEs are normally unattained. In contrast, if two or more identical DTE moieties are linked by π-conjugated organic spacers, the ring-closing reaction at one DTE unit always results in impeding photocyclization at other ring-open DTE moieties because of facile intramolecular excited energy transfer from the ring-open form to the ring-closed one that prohibits further formation of fully ring-closed species.[17−23] As a result, stepwise ring-closing reactions could not be performed in both electronically isolated and totally delocalized systems. To attain all possible ring-open/-closed isomers in a combined molecule, it is necessary to afford a suitable electronic interaction between two or several identical DTE units so that stepwise and multiplet photochromic reactions could be conducted, but rapid intercomponent energy transfer is mostly constrained.

Although all possible ring-open/-closed isomers in different photochemical quantum yields have been found in a few organic compounds with two or three DTE units,[24−28] it is envisioned that incorporating multi-DTE ligands to a metal coordinated system is another alternative approach to achieve stepwise photochromic reaction as demonstrated by one Pt(II)[29] and one Au(I)[30] complex with two identical DTE-acetylide moieties bound to a *trans*-Pt(PBu$^t_3$)$_2$ or Au(I) spacer through a Pt−acetylide or Au−acetylide bond. It has been demonstrated that incorporating DTE ligands with photo-, electro-, or magneto-active metal coordinated systems[31−42] not only allows improvement of the photoswitching functionality,

Received: August 2, 2012
Published: August 31, 2012

 © 2012 American Chemical Society dx.doi.org/10.1021/ja3076204 | J. Am. Chem. Soc. 2012, 134, 16059−16067

Scheme 1. Six States of Complex 2 from Stepwise Photochemical and Electrochemical Reactions

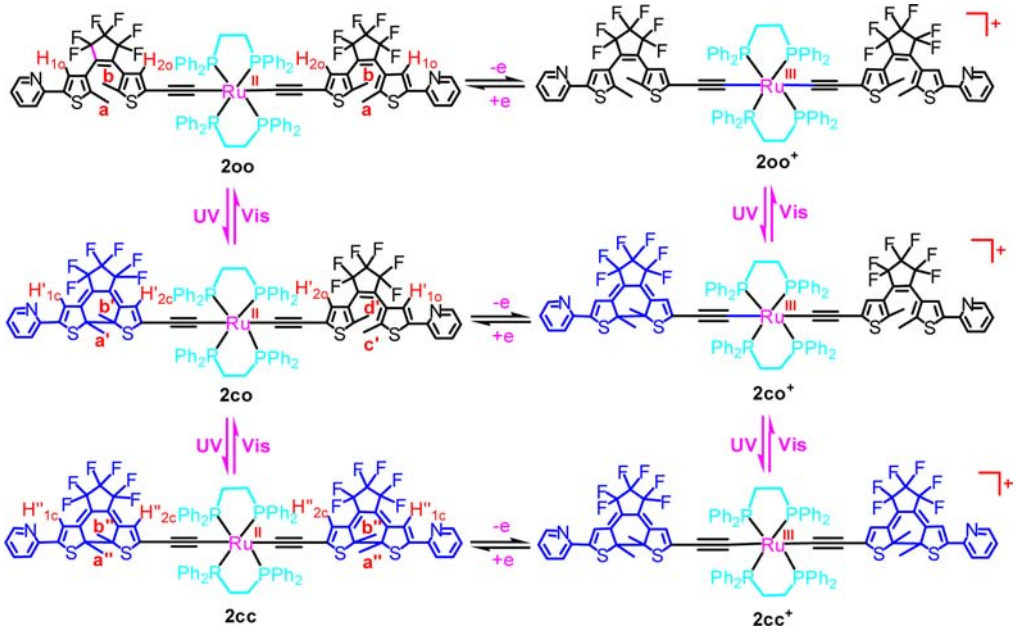

but also affords a feasible approach to modulate optical, electronic, magnetic, and catalytic properties.[3−10] With judicious selection of an electrochemically active metal coordinated system bound to two DTE moieties, it is possible to modulate stepwise photochromic reactions through reversible changes in oxidation states.

As a redox-active metal center, Ru(II) is a better electronic mediator than Pt(II) or Au(I) when two ferrocenyl-acetylides (Fc−C≡C) are bound to the metal center to give the Fc−C≡C−M−C≡C−Fc array.[43−45] It has been demonstrated that electronic communication between two ferrocenyl (Fc) units in Fc−C≡C−M−C≡C−Fc is more remarkable for M = Ru(II)[43] than that for M = Pt(II)[44] or Au(I).[45] With this in mind, Ru(II/III) coordinated system DTE−C≡C−M−C≡C−DTE was elaborately designed, taking advantage of two identical DTE-acetylides bound to *trans*-Ru(dppe)$_2$ (dppe = 1,2-bis(diphenylphosphino)ethane). We are particularly interested in two crucial issues with this system. On the one hand, when a ruthenium unit is bound to two identical DTE moieties, is it possible to overcome intramolecular energy transfer from the higher energy level of the ring-open DTE unit to the ring-closed one so that the fully ring-closed form is attained in high yield? On the other hand, is it possible to modulate stepwise and dual photocyclization reactions through the oxidation of Ru(II) to Ru(III)?

We describe herein the synthesis, characterization, and photochromic properties of ruthenium(II) complex **2oo** (Scheme 1) and its oxidized species **2oo**$^+$ with two identical DTE-acetylide units linked to a *trans*-Ru(dppe)$_2$ spacer through bis(Ru−acetylide) bonds. As expected, stepwise and dual photocyclization/cycloreversion reactions are indeed achieved for both **2oo** and its oxidized species **2oo**$^+$. The quantum yields of stepwise photochemical reactions **2oo**→**2co**→**2cc** are obviously higher than the corresponding **2oo**$^+$→**2co**$^+$→**2cc**$^+$. It is intriguing that **2oo**$^+$/**2co**$^+$/**2cc**$^+$ displays near-infrared (NIR) absorption following stepwise photocyclization reactions of two DTE units, strikingly different from **2oo**/**2co**/**2cc**.

RESULTS AND DISCUSSION

Complex **2oo** was prepared by the reaction of Ru(dppe)$_2$Cl$_2$ with 2.5 equiv of ethynyl-DTE (L1o) ligand in CH_2Cl_2 (Scheme S1) in the presence of 2.5 equiv of $NaPF_6$ and NEt_3 to afford the desired product in 64% yield. The oxidized species **2oo**$^+$ was obtained by electrochemical oxidation in an optically transparent thin-layer electrochemical (OTTLE) cell with the potential at 0.7 V in 0.2 M $(Bu_4N)(PF_6)$ dichloromethane solution at ambient temperature.

Upon irradiation under UV light at 365 nm, a colorless CH_2Cl_2 solution of L1o turned blue with the occurrence of a broad absorption band centered at 591 nm (Figure S1, Supporting Information) due to the formation of ring-closed L1c. The photocyclization and cycloreversion quantum yields of L1o and L1c are 0.41 and 0.022 (Table 1), respectively. The conversion yield of L1o→L1c is >95% at the photostationary state (PSS) as revealed by the NMR spectral studies.

Table 1. Photochemical Quantum Yields[a] and Conversion Percentage at Photostationary State (PSS)

	$\Phi_{o\rightarrow c}$[c]	$\Phi_{c\rightarrow o}$[d]	conversion at PSS[b]
L1o	0.41 (L1o→L1c)	0.022 (L1c→L1o)	>95%
2oo	0.76 (**2oo**→**2co**)	0.065	>95% (→**2co**)
	0.16 (**2co**→**2cc**)		75% (→**2cc**)
2oo$^+$	0.20 (**2oo**$^+$→**2co**$^+$)	0.033	
	0.02 (**2co**$^+$→**2cc**$^+$)		

[a]Data obtained with an uncertainty of ±10%. [b]Conversion percentages measured by NMR spectroscopy. [c]Data obtained with irradiation at 365 nm. [d]Data obtained with irradiation at 672 nm.

UV−Vis−NIR Spectral Studies. Complex **2oo** (Figure 1) exhibits a strong absorption band at ca. 313 nm due to DTE-centered transitions together with an intense absorption band at 347 nm tailing to 500 nm, arising mainly from $\pi\rightarrow\pi^*$(L1o) IL (intraligand), 4d (Ru)→π^*(dppe) MLCT, and π(L1o)→π^*(dppe) LLCT states as supported by the computational studies (vide infra). Upon irradiation of complex **2oo** with UV light at 365 nm (Figure 1), while the intense absorption bands

dx.doi.org/10.1021/ja3076204 | J. Am. Chem. Soc. 2012, 134, 16059−16067

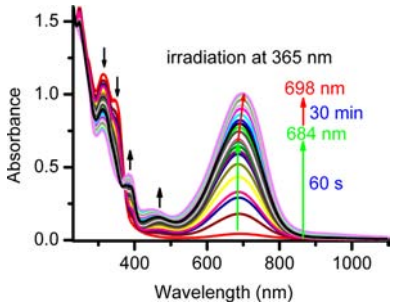

Figure 1. UV−vis−NIR absorption spectral changes of **2oo** in CH_2Cl_2 at 298 K upon irradiation at 365 nm, showing the stepwise photocyclization reactions **2oo**→**2co**→**2cc**.

at 313 and 347 nm gradually decreased, three new bands centered at 390, 470, and 684 nm occurred, which are progressively enhanced in intensity with the ongoing photocyclization reaction of one L1o to produce singly ring-closed species **2co** (Scheme 1). Meanwhile, the colorless solution turned cyan in 1 min. When the solution of singly ring-closed species **2co** was further irradiated with UV light at 365 nm for 30 min, the band centered at 684 nm continually increased in intensity and meanwhile progressively red-shifted to 698 nm due to further photocyclization reaction **2co**→**2cc** at the second L1o to L1c (Scheme 1). As depicted in Figure 1, the ring-closing absorption maximum was first observed at 684 nm and then increasingly red-shifted to 698 nm, demonstrating unambiguously that distinctly stepwise photocyclization reactions occurred indeed through **2oo**→**2co**→**2cc** (Scheme 1). Obviously, low-energy absorption at ca. 684 nm due to ring-closing reaction of one L1o to L1c is drastically red-shifted as compared to that of free ligand (591 nm, Figure S1, Supporting Information) because of the more extended π-system upon complexation with ruthenium(II) center through bis(Ru−acetylide) coordination. Relative to that in singly ring-closed **2co** (684 nm), the low-energy absorption band in dually ring-closed **2cc** (698 nm) is further red-shifted due to the better π-conjugation in the latter. On the other hand, when the solution at the photostationary state (PSS) is irradiated with the light at 672 nm (Figure S4, Supporting Information), the reversed UV−vis absorption spectral changes were observed due to corresponding stepwise cycloreversion reactions **2cc**→**2co**→**2oo**.

It is noticeable that distinct two-step UV−vis−NIR spectral changes indicate that more remarkable stepwise photocyclization occurs for Ru(II) complex **2oo** than for Pt(II)[29] or Au(I)[30] species described previously. It appears that Ru(II) as a favorable electronic mediator is a better spacer than Pt(II)[29] or Au(I)[30] to achieve stepwise photochromic reactions when multi-DTEs are incorporated through metal−acetylide bonds. It is likely that the coordination of Ru(II) center to DTE-acetylide through Ru−acetylide σ−bonding promotes intersystem crossing through metal-perturbed IL or MLCT excited state. Upon irradiation of **2oo** with the light of the wavelength at a metal-perturbed IL or MLCT absorption band (ca. 350 nm), subsequent energy transfer from the metal-based moiety toward a DTE-localized triplet excited state may occur, which may then be the photoactive state undergoing cyclization.

Complex **2oo** was readily oxidized to **2oo**$^+$ through electrochemical oxidation of Ru^{II} to Ru^{III} in dichloromethane using an OTTLE cell. The UV−vis−NIR absorption spectral changes through electrolysis of **2oo** at the potential of 0.7 V at 298 K are shown in Figure 2. The oxidized species **2oo**$^+$ exhibits a NIR band at ca. 1263 nm, ascribed mainly to the

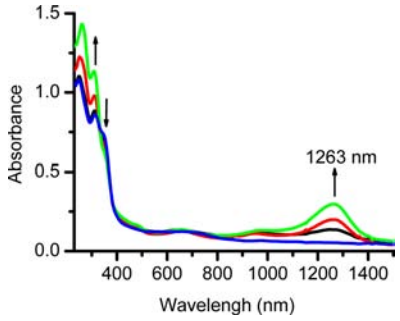

Figure 2. UV−vis−NIR spectral changes upon electrochemical oxidation of **2oo** into **2oo**$^+$ with the potential at 0.7 V in 0.2 M $(Bu_4N)(PF_6)$ dichloromethane at 298 K.

LMCT (ligand-to-metal charge transfer) transition from DTE-acetylide and dppe to the Ru(III) center.

When the solution of **2oo**$^+$ was irradiated under UV light at 365 nm, with gradual decrease of the NIR band at ca. 1263 nm, two new low-energy bands centered at 656 and 953 nm occurred progressively due to photocyclization reaction at one of the two L1o to produce singly ring-closed species **2co**$^+$ (Figure S6, Supporting Information). Upon further irradiation of the solution at 365 nm, the ring-closing absorption band at 656 nm is progressively red-shifted (Figure 3) to 670 nm due to

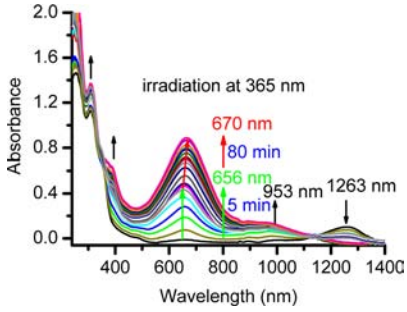

Figure 3. UV−vis−NIR spectral changes of oxidized complex **2oo**$^+$ upon irradiation at 365 nm, showing stepwise photocyclization reactions **2oo**$^+$→**2co**$^+$→**2cc**$^+$.

further photocyclization reaction at the second L1o to afford dually ring-closed species **2cc**$^+$. Meanwhile, the NIR band at 953 nm is further intensified, whereas the band at 1263 nm disappeared gradually due to the further conversion of **2co**$^+$ to **2cc**$^+$ (Figure S7, Supporting Information). Thus, the UV−vis−NIR spectral changes indicated unambiguously that stepwise photocyclization reactions **2oo**$^+$→**2co**$^+$→**2cc**$^+$ occurred indeed to give singly ring-closed species **2co**$^+$ first and then fully ring-closed product **2cc**$^+$ upon keeping irradiation under UV light at 365 nm. Conversely, when the solution at photostationary state (PSS) is irradiated with the light at 672 nm (Figure S12, Supporting Information), stepwise photocycloreversion reactions **2cc**$^+$→**2co**$^+$→**2oo**$^+$ (Scheme 1) were accordingly operated.

The NIR band in **2co**$^+$ and **2cc**$^+$ (953 nm) is distinctly blue-shifted as compared to that in **2oo**$^+$ (1263 nm), which is elucidated by their difference in transition character between ring-open **2oo**$^+$ and ring-closed **2co**$^+$/**2cc**$^+$ as suggested by computational studies (vide infra). The low-energy absorption

dx.doi.org/10.1021/ja3076204 | J. Am. Chem. Soc. 2012, 134, 16059−16067

in visible region due to ring-closed L1c also shows a significant blue-shift in oxidized complex **2co**$^+$ (656 nm) or **2cc**$^+$ (670 nm) as compared to that in **2co** (684 nm) or **2cc** (698 nm). The quantum yields of photochromic reactions for **2oo** and **2oo**$^+$ are depicted in Table 1. The much higher photocyclization quantum yield of **2oo**→**2co** (Φ = 0.76) than L1o→L1c (Φ = 0.41) in free ligand is mostly ascribed to the electron-rich character of Ru(II) center bound to two DTE units. In contrast, the lower photocyclization quantum yields of **2oo**$^+$→**2co**$^+$ (Φ = 0.20) and **2co**$^+$→**2cc**$^+$ (Φ = 0.02) than those of **2oo**→**2co** (Φ = 0.76) and **2co**→**2cc** (Φ = 0.16) are mostly due to the electron-deficient nature of the Ru(III) center. Undoubtedly, the lower electronic density at the reactive carbon atoms in oxidized species **2oo**$^+$/**2co**$^+$ causes the ring-closing reaction to have more difficulty proceeding than that in **2oo**/**2co**. For stepwise photocyclization reactions **2oo**→**2co** (Φ = 0.76)→**2cc** (Φ = 0.16), the much higher quantum yield in the first step than that in the second step reveals that ring-closing reaction at one L1o impedes significantly photocyclization at the other L1o with lower conversion for **2co**→**2cc** (75%) in the second step than that for **2oo**→**2co** (>95%) in the first step. The quantum yield of cycloreversion reaction is 0.065 for **2cc** and 0.033 for **2cc**$^+$, both of which are obviously improved relative to free ligand L1c (Φ = 0.022) due to coordination to Ru(II) or Ru(III) center, thus promoting photochromic sensitivity.

NMR Spectral Studies. When **2oo** in $CDCl_3$ was irradiated with UV light at 365 nm, the ^{1}H NMR spectral signals (Figure 4a) at 7.56 ppm for H_{1o} and 6.26 ppm for H_{2o} were gradually weakened, whereas four new signals at 7.58 ppm for H_{1o}', 6.90 ppm for H_{1c}', 6.34 ppm for H_{2o}', and 5.21 ppm for H_{2c}' were increasingly enhanced following the photocyclization reaction of **2oo**→**2co** (Scheme 1). Upon keeping irradiation at 365 nm (Figure 4b) to the PSS, while the signals at 7.58 ppm for H_{1o}', 6.34 ppm for H_{2o}', 6.90 ppm for H_{1c}', and 5.21 ppm for H_{2c}' gradually decreased, two new peaks at 6.93 ppm for H_{1c}'' and 5.28 ppm for H_{2c}'' appeared increasingly, implying a further ring-closure of singly ring-closed **2co** to dually ring-closed **2cc**. As depicted in Scheme 1 and Figure 4, the changes of CH_3 protons also demonstrated the occurrence of stepwise ring-closing reactions **2oo**→**2co**→**2cc**. The signals of CH_3 protons in **2oo** were observed at 1.97 (methyl *b*) and 1.83 ppm (methyl *a*) (Figure 4a). Upon irradiation of **2oo** at 365 nm, the two methyl signals were gradually attenuated with the occurrence of two new low-field shifted signals at 2.19 ppm (methyl *b*′) and 2.17 ppm (methyl *a*′) together with another two new methyl signals at 1.98 ppm (methyl *d*′) and 1.85 ppm (methyl *c*′) with a slight low-field shift relative to methyl signals *b* (1.97 ppm) and *a* (1.83), suggesting the occurrence of **2oo**→**2co** conversion due to the photocyclization reaction of one of the two DTE moieties (Figure 4a). Further keeping irradiation at 365 nm resulted in gradual reduction in intensity for both sets of methyl signals of **2co** (signals *a*′, *b*′ and *c*′, *d*′), whereas two new overlapped methyl signals *b*″ and *a*″ at 2.20 and 2.18 ppm were observed because of further photocyclization of the second DTE to produce the dually ring-closed form **2cc** (Figure 4b).

Stepwise photochromic reactions were unambiguously supported by ^{31}P NMR spectral studies (Figure 5). When a

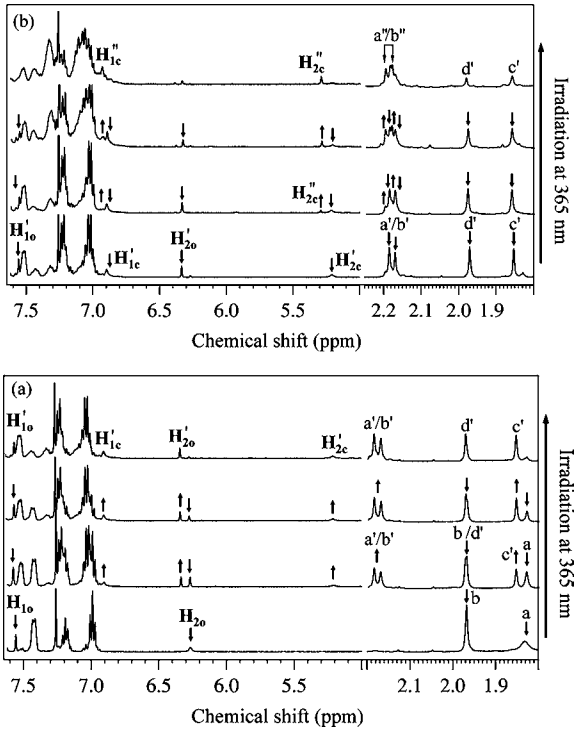

Figure 4. ^{1}H NMR spectral changes of **2oo** in $CDCl_3$ upon irradiation at 365 nm to the PSS, showing the conversion of (a) **2oo**→**2co** and (b) **2co**→**2cc**.

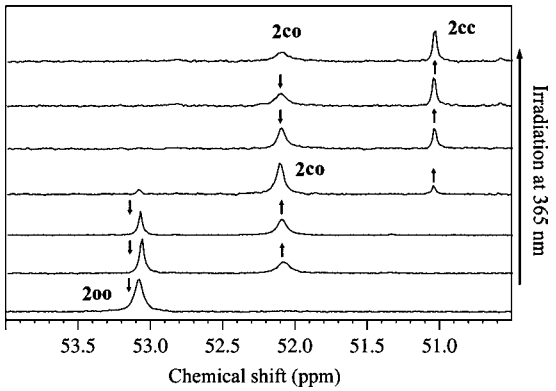

Figure 5. ^{31}P NMR spectral changes of **2oo** in $CDCl_3$ upon irradiation at 365 nm, showing stepwise conversion **2oo**→**2co**→**2cc**.

$CDCl_3$ solution of **2oo** was irradiated at 365 nm, the P signal at 53.08 ppm decreased gradually and vanished finally, whereas a new P signal was first observed at 52.09 ppm due to the photocyclization reaction of one of the two ring-open L1o to give **2co**. When the solution of **2co** was further irradiated with UV light at 365 nm, the P signal at 52.09 ppm for **2co** decreased gradually, whereas a new peak occurred at 51.04 ppm due to the photocyclization reaction of the second ring-open L1o to produce dually ring-closed **2cc**. From the ^{31}P NMR spectral changes, the contents of **2oo**, **2co**, and **2cc** against irradiation time are estimated as shown in Figure 6. It is revealed that **2oo** was first converted to **2co** quickly and then to **2cc** slowly upon irradiation at 365 nm so that singly ring-closed intermediate **2co** was successfully accessed with ca. 85% of maximum percentage. At the PSS, the P signal integral ratio between **2co** (52.09 ppm) and **2cc** (51.04 ppm) suggested the presence of ca. 25% of **2co** and 75% of **2cc** (Figure 6).

Electrochemical Studies. The electrochemical data of **2oo**, **2co**, and **2cc** versus Ag/AgCl in 0.1 M $(Bu^n_4N)(PF_6)$-

dx.doi.org/10.1021/ja3076204 | J. Am. Chem. Soc. 2012, 134, 16059−16067

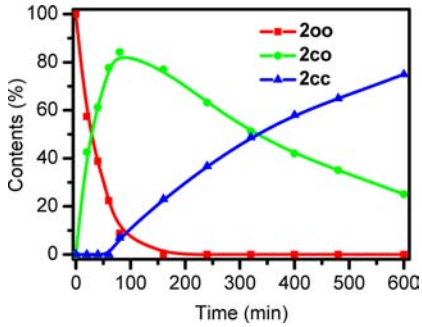

Figure 6. Relative contents of **2oo** (red), **2co** (green), and **2cc** (blue) under UV light irradiation at 365 nm, revealed from ^{31}P NMR spectral studies in $CDCl_3$ solution.

dichloromethane solutions are summarized in Table 2. The electrochemical behavior of **2oo** was in situ monitored under

Table 2. Electrochemical Data of 2oo, 2co, and 2cc versus Ag/AgCl in 0.1 M $(Bu^n_4N)(PF_6)$-Dichloromethane Solutions

	$E_{1/2}$ (ΔE_p)^{a,b}	
	Ru-centered	DTEs
2oo	0.52 (0.07)	1.29 (E_a)^c
2co	0.47 (0.08)	0.95 (0.10), 1.23 (0.13)
2cc	0.49 (0.09)	0.85 (0.08), 1.04 (0.08)

[a]Potential data in volts vs Ag/AgCl are from single scan cyclic voltammograms recorded at 25 °C in 0.1 M dichloromethane solution of $(Bu_4N)(PF_6)$. Detailed experimental conditions are given in the Experimental Section. [b]ΔE_p denotes the difference between the anodic and cathodic potentials from cyclic voltammogram. [c]E_a is anodic potential.

UV irradiation at 365 nm using cyclic and differential pulse voltammetry. The plots of cyclic voltammogram (CV) and differential pulse voltammogram (DPV) in 0.1 M $(Bu_4N)(PF_6)$ dichloromethane solutions are shown in Figure 7. Complex **2oo** displays a reversible wave at 0.52 V (vs Ag/AgCl) due to the oxidation of Ru(II) to Ru(III) together with a quasi-reversible wave at 1.29 V, resulting most likely from the L1o-centered oxidation process because free L1o exhibits similar electrochemical behavior in this potential. When singly ring-closed species **2co** was formed upon irradiation of **2oo** with UV light at 365 nm, both waves at 0.52 and 1.29 V gradually decreased and finally disappeared (Figure S13a, Supporting Information), while three new oxidation waves were observed at 0.47, 0.95, and 1.23 V (vs Ag/AgCl), respectively. The wave at 0.47 V is due to the Ru^{II}-centered oxidation process of **2co**, which shows some negative potential shift (0.05 V) relative to **2oo** (0.52 V). The waves at 0.95 and 1.23 V are assigned to one ring-closed L1c and the other ring-open L1o in **2co**, respectively, in which the oxidation potential of ring-closed L1c (0.95 V) is distinctly lower than ring-open L1o (1.23 V) due to the better π-conjugation in ring-closed DTE. Upon further irradiation of singly ring-closed species **2co** with UV light at 365 nm, the waves at 0.95 and 1.23 V were gradually reduced (Figure S13b, Supporting Information), whereas two new waves at 0.85 and 1.04 V occurred progressively due to the sequential oxidation of two ring-closed DTEs in **2cc**. A stepwise oxidation of two identical L1c in **2cc** with potential difference $\Delta E_{1/2}$ = 0.19 V (Figure 7b) and corresponding comproportionation constant $K_c = \exp(\Delta E_{1/2}/25.69)$ = 1629 implies that significant electronic communication[46] is substantially trans-

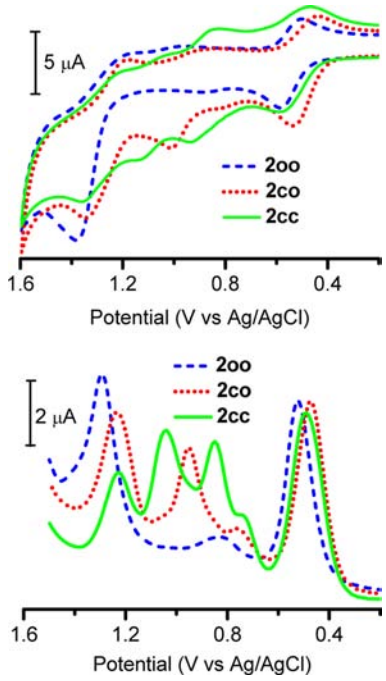

Figure 7. Plots of cyclic voltammogram (top) and differential pulse voltammogram (lower) of **2oo** (blue), **2co** (red), and **2cc** (green) in 0.1 M $(Bu_4N)(PF_6)$ dichloromethane upon irradiation at 365 nm.

mitted between the two L1c across the *trans*-$Ru(dppe)_2$ moiety. Such a large electronic interaction between two identical L1c in **2cc** ($\Delta E_{1/2}$ = 0.19 V) is comparable to that between two Fc in *trans*-$Ru(dppe)_2(C{\equiv}C{-}Fc)_2$ ($\Delta E_{1/2}$ = 0.205 V),[43] but larger than that between two TTF in *trans*-$[Ru(C{\equiv}CMe_3TTF)_2(dppe)_2]$[47a] ($\Delta E_{1/2}$ = 0.11 V, $HC{\equiv}CMe_3TTF$ = 4-ethynyl-trimethyltetrathiafulvalene) across the *trans*-$Ru(dppe)_2$ spacer. This is obviously more pronounced than electronic communication between two identical DTE-acetyldes across the *trans*-$Pt(PBu^t_3)_2$ moiety in the DTE−C≡C−$Pt(PBu^t_3)_2$−C≡C−DTE compound.[29]

IR Spectra Studies. The IR band of the C≡C stretching mode in **2oo** is located at 2055 cm^{-1} in CH_2Cl_2 solution (Figure S14, Supporting Information). When the solution of **2oo** was irradiated under UV light at 365 nm, the ν(C≡C) band at 2055 cm^{-1} was first red-shifted to 2015 cm^{-1} with the conversion of **2oo** to **2co** (Figure S14a, Supporting Information), and then further red-shifted to 2010 cm^{-1} upon singly ring-closed **2co** being converted to fully ring-closed **2cc** (Figure S14b, Supporting Information). A progressive red-shift of the ν(C≡C) is ascribed to the increased π-system with stepwise photocyclization reactions **2oo**→**2co**→**2cc** so that π electron density of the acetylide is largely delocalized to whole coordinated system, thus attenuating the C≡C bonding.

With the electrochemical oxidation of **2oo** into $\mathbf{2oo}^+$ in dichloromethane using an OTTLE cell, the ν(C≡C) band at 2055 cm^{-1} was significantly red-shifted to 1947 cm^{-1} because electronic density of the acetylide is remarkably reduced upon the oxidation of Ru^{II} to Ru^{III}. When the solution of $\mathbf{2oo}^+$ is irradiated under UV light at 365 nm, the ν(C≡C) band at 1947 cm^{-1} is slightly red-shifted to 1943 cm^{-1}, and then further to 1941 cm^{-1} with stepwise ring-closing reactions $\mathbf{2oo}^+$→$\mathbf{2co}^+$→$\mathbf{2cc}^+$ (Figure S16, Supporting Information). Obviously, the stepwise ring-closure-triggered red-shift of the ν(C≡C)

dx.doi.org/10.1021/ja3076204 | J. Am. Chem. Soc. 2012, 134, 16059−16067

band in **2oo** is much more remarkable than that in the oxidized species **2oo**$^+$, coinciding with the trend observed in the UV−vis spectral studies.

Computational Studies. TD-DFT computational studies have been performed on six ring-open/closed isomers (Tables S1−S6). The HOMO of **2oo** is distributed on Ru(II) center and two L1o, while the LUMO is mainly resident on one ring-open L1o. The low-energy absorption arises primarily from $\pi\rightarrow\pi^*$ (L1o) IL and 4d (Ru)$\rightarrow\pi^*$ (dppe) MLCT transitions, mixed with some π(L1o)$\rightarrow\pi^*$(dppe) LLCT state. For **2co**, both the HOMO and the LUMO are mostly contributed by the ring-closed L1c (77% for HOMO and 93% for LUMO). The low-energy absorption of **2co** is featured with the $\pi\rightarrow\pi^*$ (L1c) IL transition from ring-closed L1c, mixed with some 4d(Ru)$\rightarrow\pi^*$(L1c) MLCT state. For **2cc**, the HOMO is uniformly distributed on two ring-closed L1c and Ru(II) centers, while the LUMO is mainly localized on one ring-closed L1c. The low-energy absorption results primarily from $\pi\rightarrow\pi^*$ (L1c) IL and π(L1c)$\rightarrow\pi^*$(L1c′) LLCT states, mixed with a minor contribution from the 4d(Ru)$\rightarrow\pi^*$(L1c) MLCT state. A remarkable LLCT character from one ring-closed L1c to the other ring-closed L1c′ in **2cc** is experimentally reflected by significant electronic communication between two ring-closed L1c as revealed from electrochemical studies.

The oxidized species **2oo**$^+$/**2co**$^+$/**2cc**$^+$ have two groups of orbitals (α and β) due to the unpaired electron in the unrestricted calculations. The calculated NIR absorption of **2oo**$^+$ is mainly featured with LMCT transition from ring-open L1o and dppe to Ru(III). For **2co**$^+$, the NIR absorption is mainly assigned to the LLCT state from ring-open L1o to ring-closed L1c, mixed with some LMCT character from ring-open L1o to Ru(III). The low-energy band in the visible region is primarily featured with IL transition within ring-closed L1c, mixed with minor character of LLCT state from ring-open L1o to ring-closed L1c. For **2cc**$^+$, the calculated NIR absorption is ascribed to LLCT transition from one ring-closed L1c to the other ring-closed L1c′, mixed with some LMCT transition from L1c to Ru(III). The low-energy absorption band in the visible region is featured with the L1c-centered IL transition, mixed with some LLCT character from one L1c to the other L1c′. A distinct blue-shift of the NIR bands in **2co**$^+$ and **2cc**$^+$ relative to that in **2oo**$^+$ is probably elucidated by their difference in transition character. The NIR band in **2oo**$^+$ arises primarily from the π(L1o/dppe)$\rightarrow$4d(Ru) LMCT state, whereas that in **2co**$^+$ or **2cc**$^+$ is mostly contributed by π(L1o/L1c) $\rightarrow\pi^*$(L1c′) LLCT transitions mixed with some LMCT character.

As shown in Figure 8, the energy levels of frontier molecular orbitals involving in ring-closing transitions of L1c are much lower in electron-deficient Ru(III) species **2cc**$^+$ than those in electron-rich complex **2cc**. The transition energy of 1.93 eV corresponding to the dually ring-closing absorption due to βHOMO−3$\rightarrow\beta$LUMO and βHOMO−5$\rightarrow\beta$LUMO in **2cc**$^+$ (Table S6, Supporting Information) is distinctly larger than that of 1.83 eV due to HOMO$\rightarrow$LUMO, HOMO$\rightarrow$LUMO+1, HOMO−1$\rightarrow$LUMO, and HOMO−1$\rightarrow$LUMO+1 in **2cc** (Table S3, Supporting Information). Thus, ring-closing absorption bands of L1c in **2cc**$^+$ show an obvious blue-shift relative to **2cc** upon oxidation of Ru(II) to Ru(III) as demonstrated experimentally, in which the measured ring-closing absorption at 698 nm (**2cc**) is obviously blue-shifted to 670 nm (**2cc**$^+$).

From TD-DFT studies, it is found that the unpaired electron in **2oo**$^+$ (Figure S27, Supporting Information) is mainly localized onto the bis(acetylide)-Ru(III) moiety. When **2oo**$^+$ is converted to **2co**$^+$, the spin density is distributed on the ring-closed L1c and Ru(III) center. For **2cc**$^+$, the spin density is delocalized over the entire molecule with significant inhabitant on two L1c and Ru(III) center. A stability study was performed, and the plots of $\ln(A/A_0)$ versus time for the absorbance decay of **2oo**$^+$ at 1263 nm and **2co**$^+$/**2cc**$^+$ at 953 nm are shown in Figure S28 (Supporting Information). It is revealed that **2oo**$^+$/**2co**$^+$/**2cc**$^+$ undergo slow decay in CH_2Cl_2 solution at room temperature with the stability following **2oo**$^+$ < **2co**$^+$ < **2cc**$^+$, coinciding well with the increasingly enhanced delocalization of the unpaired electron.

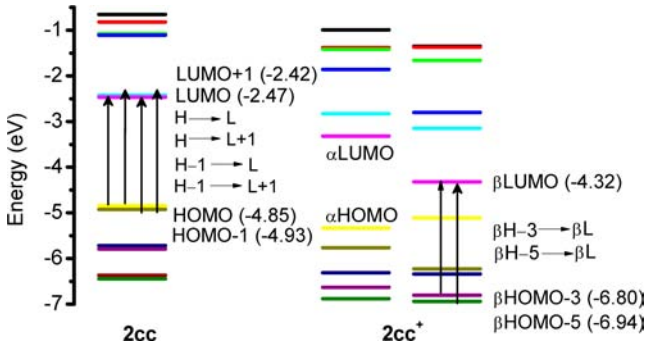

Figure 8. Energy levels of frontier molecular orbitals and the transitions due to ring-closing of L1 in **2cc** and oxidized product **2cc**$^+$.

CONCLUSIONS

Bis(σ-acetylide) ruthenium(II) complex **2oo** and its oxidized ruthenium(III) species **2oo**$^+$ with two identical DTE-acetylides are elaborately designed and prepared. Both complexes exhibit distinctly stepwise photochromic reactions, which could be modulated by reversible oxidation/reduction of Ru(II) ⇆ Ru(III). It is found that stepwise photochemical conversion percentage and quantum yield in **2oo** are much higher than those in its oxidized complex **2oo**$^+$, ascribed to the reduced electronic density at the reactive carbon atoms upon the oxidation of Ru(II) to Ru(III). Electrochemical studies indicate that a significant electronic interaction is operating between two identical DTE units spaced by *trans*-Ru(dppe)$_2$ in dually ring-closed **2cc**/**2cc**$^+$. It is demonstrated that stepwise photochromism in a coordination system with two identical DTE-acetylides bound to a Ru(II) center is more remarkable than that bonded to a Pt(II)[29] or Au(I)[30] center described previously.

EXPERIMENTAL SECTION

General Procedures and Materials. All of the synthetic procedures were carried out by using Schlenk techniques and vacuum-line systems under a dry argon atmosphere unless otherwise specified. Solvents were distilled under argon atmosphere in the presence of sodium and benzophenone (THF) or calcium hydride (dichloromethane and methanol). *cis*-Ru(dppe)$_2$Cl$_2$[47a,b] and 3-bromo-2-methyl-5-thienyl boronic acid[47c] were prepared according to the literature procedures. Other chemicals were commercially available and used as received without further purification.

2-(2′-Pyridyl)-4-bromo-5-methylthiophene. 2-Bromopyridine (1.9 g, 0.012 mol), 3-bromo-2-methyl-5-thienyl boronic acid (2.2 g, 0.01 mol), and tetrakis(triphenylphosphine) palladium(0) (0.8 g, 0.68 mmol) were dissolved in THF (80 mL). Upon stirring for 15 min, an aqueous (30 mL) solution of sodium carbonate (6.4 g, 60 mmol) was added. The mixture was vigorously stirred under reflux, and the reaction was monitored by TLC. The product was extracted with

dx.doi.org/10.1021/ja3076204 | J. Am. Chem. Soc. 2012, 134, 16059−16067

diethyl ether, dried with $MgSO_4$, and concentrated under reduced pressure. The residue was purified by column chromatography on silica gel using dichloromethane−petroleum (2:1, v/v) as eluent. Yield: 84% (2.1 g). ^{1}H NMR (DMSO, ppm): δ 8.52−8.51 (m, 1H), 7.91 (d, J = 8.0 Hz, 1H), 7.82 (td, J_1 = 7.72 Hz, J_2 = 1.32 Hz, 1H), 7.76 (s, 1H), 7.29−7.26 (m, 1H), 2.39 (s, 3H). ESI-MS: m/z (%) 253 (100) $[M]^+$.

1-(5-Methyl-2-(2′-pyridyl)-4-thienyl)perfluorocyclopentene. 2-(2′-Pyridyl)-4-bromo-5-methylthio-phene (1.27 g, 5.0 mmol) was dissolved in dry THF (30 mL) under argon atmosphere. The solution was cooled to −78 °C, to which was slowly added *n*-butyllithium (1.6 M in hexane, 3.3 mL, 5.25 mmol). Upon stirring at −78 °C for 1 h, perfluorocyclopentene (0.68 mL, 5.0 mmol) was added quickly. The solution was stirred at −78 °C for 2 h, and then put aside at ambient temperature. A dilute HCl aqueous solution was added to the reaction mixture, which was then extracted with diethyl ether for three times. The combined organic layer was dried with $MgSO_4$, and then filtered and evaporated in vacuo. The residue was purified by column chromatography on silica gel using dichloromethane−petroleum ether (v/v = 1:2) as eluent. Yield: 73% (1.24 g). ^{1}H NMR ($CDCl_3$, ppm): δ 8.57−8.55 (m, 1H), 7.71 (td, J_1 = 7.56 Hz, J_2 = 1.72 Hz, 1H), 7.63 (d, J = 8.0 Hz, 1H), 7.51 (s, 1H), 7.20−7.16 (m, 1H), 2.50 (d, J = 3.12 Hz, 3H). ESI-MS: m/z (%) 368 (100) $[M + H]^+$.

Synthesis of 1-(5-Methyl-2-(2′-pyridyl)-4-thienyl)-2-(2-methyl-5-trimethylsilylethynyl-3-thienyl)perfluorocyclopentene. When a dry THF (40 mL) solution of 3-bromo-2-methyl-5-trimethylsilyl-ethynylthiophene (548 mg, 2 mmol) was cooled to −78 °C, *n*-butyllithium (1.6 M in hexane, 1.3 mL, 2.1 mmol) was added slowly to the solution. Upon stirring at −78 °C for 30 min, to the solution was added 1-(5-methyl-2-(2′-pyridyl)-4-thienyl) perfluorocyclopentene (734 mg, 2 mmol) dissolved in dry THF (5 mL). After the reaction mixture was stirred at −78 °C for 2 h, dilute hydrochloric acid was added. The product was extracted with diethyl ether, which was dried with $MgSO_4$ and then concentrated under reduced pressure. The residue was purified by silica gel column chromatography using dichloromethane−petroleum ether (v/v = 1:1) as eluent to afford the product as pale blue oil. Yield: 68% (735 mg). ^{1}H NMR ($CDCl_3$, ppm): δ 8.55 (d, J = 7.88 Hz, 1H), 7.71 (td, J_1 = 7.72 Hz, J_2 = 1.52 Hz, 1H), 7.62 (d, J = 7.96 Hz, 1H), 7.51 (s, 1H), 7.24 (s, 1H), 7.18 (dd, J_1 = 7.28 Hz, J_2 = 4.80 Hz, 1H), 1.95 (s, 3H), 1.89 (s, 3H), 0.25 (s, 9H). ESI-MS: m/z (%) 542.4 (100) $[M + H]^+$.

Synthesis of 1-(5-Methyl-2-(2′-pyridyl)-4-thienyl)-2-(2-methyl-5-ethynyl-3-thienyl)-perfluorocyclopentene (L1o). To a THF−methanol (40 mL, v/v = 1:1) solution of 1-(5-methyl-2-(2′-pyridyl)-4-thienyl)-2-(2-methyl-5-trimethylsilylethynyl-3-thienyl)-perfluorocyclopentene (542 mg, 1 mmol) was added excess of anhydrous potassium carbonate. Upon stirring overnight, the solution was concentrated, to which water was added. The product was extracted with ethyl acetate, dried with anhydrous $MgSO_4$, and concentrated under reduced pressure. The residue was purified by chromatography on a silica gel column using dichloromethane−petroleum ether (v/v = 2:1) as eluent to afford to the product as pale blue oil. Yield: 92% (431 mg). ^{1}H NMR ($CDCl_3$, ppm): δ 8.55 (d, J = 4.32 Hz, 1H), 7.71 (td, J_1 = 8 Hz, J_2 = 1.72 Hz, 1H), 7.63 (d, J = 8 Hz, 1H), 7.51 (s, 1H), 7.28 (s, 1H), 7.18 (dd, J_1 = 7.42 Hz, J_2 = 4.80 Hz, 1H), 3.36 (s, 1H), 1.94 (s, 3H), 1.92 (s, 3H). ESI-MS: m/z (%) 470 (100) $[M + H]^+$.

Synthesis of Complex 2oo. *cis*-Ru(dppe)$_2$Cl$_2$ (96.8 mg, 0.1 mmol) and L1o (117 mg, 0.25 mmol) were dissolved in dichloromethane (40 mL), and then $NaPF_6$ (42 mg, 0.25 mmol) and triethylamine (60 μL) were added. After the mixture was stirred at ambient temperature for 8 h, the solvent was removed under vacuum. The residue was purified by chromatography on a short alumina column using CH_2Cl_2 as eluent. The product was recrystallized in dichloromethane−hexane solution to give a pale green solid. Yield: 64% (116 mg). ^{1}H NMR ($CDCl_3$, ppm): δ 8.56 (d, J = 4.64 Hz, 2H), 7.67 (td, J_1 = 7.44 Hz, J_2 = 1.56 Hz, 2H), 7.63 (d, J = 7.88 Hz, 2H), 7.56 (s, 2H), 7.43−6.97 (m, 40H), 7.04 (t, J = 8.0 Hz, 2H), 6.26 (s, 2H), 2.57 (s, 8H), 1.97 (s, 6H), 1.83 (s, 6H). ^{13}C NMR ($CDCl_3$, ppm): 149.6, 136.8, 136.5, 134.6, 134.4, 134.0, 133.9, 133.6, 129.0, 128.8, 128.7, 127.2, 127.1, 127.0, 126.4, 124.1, 122.3, 122.1, 118.5, 31.3 (P(CH_2)$_2$P), 14.8 (CH_3). ^{31}P NMR ($CDCl_3$, ppm): δ 53.1. ESI-MS: m/z (%) 1857 (80%) $[M + Na]^+$, 1366 (100%) $[M - L1o]^+$. Anal. Calcd for $C_{96}H_{72}F_{12}N_2P_4RuS_2$: C, 62.84; H, 3.96; N, 1.51. Found: C, 62.69; H, 4.08; N, 1.53. IR (CH_2Cl_2): 2055 cm^{-1} (C≡C).

Physical Measurements. ^{1}H and ^{31}P NMR spectra were performed on a Bruker Avance III (400 MHz) spectrometer with $SiMe_4$ as the internal reference and H_3PO_4 as the external reference, respectively. UV−vis absorption spectra were measured on a Perkin-Elmer Lambda 25 UV−vis spectrophotometer. The UV−vis−NIR spectra were measured on a Perkin-Elmer Lambda 900 UV−vis−NIR spectrometer. Infrared spectra (IR) were recorded on a Magna 750 FT-IR spectrophotometer. Elemental analyses (C, H, and N) were carried out on a Perkin-Elmer model 240 C elemental analyzer. Electrospray ionization mass spectrometry (ESI-MS) was recorded on a Finnigan DECAX-30000 LCQ mass spectrometer using dichloromethane−methanol as mobile phases. UV light was produced using a ZF5 UV lamp (365 nm), and visible light irradiation (672 nm) was carried out by using a LZG220 V 1 kW tungsten lamp with cutoff filters. The quantum yields were determined by comparing the reaction yields of the diarylethenes relative to 1,2-bis(2-methyl-5-phenyl-3-thienyl)perfluorocyclopentene.[48]

The cyclic voltammogram (CV) and differential pulse voltammogram (DPV) were measured using a potentiostat/galvanostat model 263A in dichloromethane solutions containing 0.1 M (Bu_4N)(PF_6) as the supporting electrolyte. CV was performed at a scan rate of 100 mV s^{-1} and DPV at a rate of 20 mV s^{-1} with a pulse height of 40 mV. Platinum and glassy graphite were used as the counter and working electrodes, respectively, and the potential was measured against Ag/AgCl reference electrode. Controlled-potential electrolyses were performed in a two-compartment electrochemical cell with a glass frit junction of fine porosity under argon atmosphere. The UV−vis−NIR spectra of oxidized species were measured in an optically transparent thin-layer electrochemical cell (OTTLE) with the potential at ca. 0.7 V in 0.2 M (Bu_4N)(PF_6) dichloromethane at 298 K.

Theoretical Methodology. The ground-state geometries of **2oo**, **2co**, **2cc**, **2oo**$^+$, **2co**$^+$, and **2cc**$^+$ as isolated molecules were optimized using density functional theory (DFT)[49a] with the gradient corrected correlation functional PBE1PBE.[49b] In the optimization processes, the convergent values of maximum force, root-mean-square (rms) force, maximum displacement, and rms displacement were set by default. To analyze the spectroscopic properties, 80 simple excited states of the studied complexes were calculated by TD-DFT[50] method with the same functional used in the optimization processes considering the dichloromethane solution on the basis of the optimized geometrical structures. The solvent effects were taken into account by the polarizable continuum model method (PCM).[51] The self-consistent field (SCF) convergence criteria of rms density matrix and maximum density matrix were set at 10^{-8} and 10^{-6} au, respectively, in all of the electronic structure calculations. The iterations of excited states continued until the changes on energies of states were no more than 10^{-7} au between the iterations, and then convergences were reached in all of the excited states. In these calculations, the SDD[52] basis set consisting of the effective core potentials (ECP) was employed for the ruthenium, phosphorus, and sulfur atoms, and the 6-31G(p,d) basis set for the remaining atoms was used. To precisely describe the molecular properties, one additional d-type polarization function was implemented for phosphorus (α_d = 0.34) and sulfur (α_d = 0.421) atoms,[53a] and the f-type polarization function was implemented for the ruthenium (α_f = 1.235) atom.[53b] All calculations were performed with the Gaussian 03 program package.[54]

■ ASSOCIATED CONTENT

Supporting Information

Tables and figures giving additional spectroscopic, electrochemical, and computational data. This material is available free of charge via the Internet at http://pubs.acs.org.

AUTHOR INFORMATION

Corresponding Author

czn@fjirsm.ac.cn

Notes

The authors declare no competing financial interest.

ACKNOWLEDGMENTS

We are grateful for financial support from the NSFC (20931006, U0934003, and 91122006) and the NSF of Fujian Province (2011J01065).

REFERENCES

(1) Irie, M. *Chem. Rev.* **2000**, *100*, 1685.
(2) (a) Tian, H.; Yang, S. J. *Chem. Soc. Rev.* **2004**, *33*, 85. (b) Tian, H.; Wang, S. *Chem. Commun.* **2007**, 781. (c) Tian, H.; Feng, Y. *J. Mater. Chem.* **2008**, *18*, 1617.
(3) Ko, C.-C.; Yam, V. W.-W. *J. Mater. Chem.* **2010**, *20*, 2063.
(4) (a) Kume, S.; Nishihara, H. *Dalton Trans.* **2008**, 3260. (b) Uchida, K.; Yamanoi, Y.; Yonezawa, T.; Nishihara, H. *J. Am. Chem. Soc.* **2011**, *133*, 9239.
(5) Akita, M. *Organometallics* **2011**, *30*, 43.
(6) Hasegawa, Y.; Nakagawa, T.; Kawai, T. *Coord. Chem. Rev.* **2010**, *254*, 2643.
(7) Browne, W. R. *Coord. Chem. Rev.* **2008**, *252*, 2470.
(8) Gust, D.; Andreasson, J.; Pischel, U.; Moore, T. A.; Moore, A. L. *Chem. Commun.* **2012**, *48*, 1947.
(9) Klajn, R.; Stoddart, J. F.; Grzybowski, B. A. *Chem. Soc. Rev.* **2010**, *39*, 2203.
(10) Guerchais, V.; Ordronneau, L.; Bozec, H. L. *Coord. Chem. Rev.* **2010**, *254*, 2533.
(11) Perrier, A.; Maurel, F.; Jacquemin, D. *Acc. Chem. Res.* **2012**, *45*, 1173.
(12) Kobatake, S.; Kuma, S.; Irie, M. *J. Phys. Org. Chem.* **2007**, *20*, 960.
(13) Zhong, Y.-W.; Vila, N.; Henderson, J. C.; Abruna, H. D. *Inorg. Chem.* **2009**, *48*, 7080.
(14) Areephong, J.; Logtenberg, H.; Browne, W. R.; Feringa, B. L. *Org. Lett.* **2010**, *12*, 2132.
(15) Kim, H. J.; Jang, J. H.; Choi, H.; Lee, T.; Ko, J.; Yoon, M.; Kim, H.-J. *Inorg. Chem.* **2008**, *47*, 2411.
(16) Zhao, H.; Al-Atar, U.; Pace, T. C. S.; Bohne, C.; Branda, N. R. *J. Photochem. Photobiol., A: Chem.* **2008**, *200*, 74.
(17) Jung, I.; Choi, H.; Kim, E.; Lee, C.-H.; Kanga, S. O.; Ko, J. *Tetrahedron* **2005**, *61*, 12256.
(18) Perrier, A.; Maurel, F.; Jacquemin, D. *J. Phys. Chem. C* **2011**, *115*, 9193.
(19) Wong, H.-L.; Tao, C.-H.; Zhu, N.; Yam, V. W.-W. *Inorg. Chem.* **2011**, *50*, 471.
(20) Yam, V. W.-W.; Lee, J. K.-W.; Ko, C.-C.; Zhu, N. *J. Am. Chem. Soc.* **2009**, *131*, 912.
(21) Higashiguchi, K.; Matsuda, K.; Tanifuji, N.; Irie, M. *J. Am. Chem. Soc.* **2005**, *127*, 8922.
(22) Higashiguchi, K.; Matsuda, K.; Irie, M. *Angew. Chem., Int. Ed.* **2003**, *42*, 3537.
(23) Tian, H.; Chen, B.; Tu, H.; Mullen, K. *Adv. Mater.* **2002**, *14*, 918.
(24) Choi, H.; Jung, I.; Song, K. H.; Song, K.; Shin, D.-S.; Kang, S. O.; Ko, J. *Tetrahedron* **2006**, *62*, 9059.
(25) Kobatake, S. S.; Irie, S. *Tetrahedron* **2003**, *59*, 8359.
(26) Areephong, J.; Browne, W. R.; Feringa, B. L. *Org. Biomol. Chem.* **2007**, *5*, 1170.
(27) Matsuda, K.; Irie, M. *J. Am. Chem. Soc.* **2001**, *123*, 9896.
(28) Kobatake, S.; Kuma, S.; Irie, M. *Bull. Chem. Soc. Jpn.* **2004**, *77*, 945.
(29) (a) Roberts, M. N.; Carling, C.-J.; Nagle, J. K.; Branda, N. R.; Wolf, M. O. *J. Am. Chem. Soc.* **2009**, *131*, 16644. (b) Perrier, A.; Maurel, F.; Ciofini, I.; Jacquemin, D. *Chem. Phys. Lett.* **2011**, *502*, 77.
(30) Li, B.; Wu, Y.-H.; Wen, H.-M.; Shi, L.-X.; Chen, Z.-N. *Inorg. Chem.* **2012**, *51*, 1933.
(31) Liu, Y.; Lagrost, C.; Costuas, K.; Tchouar, N.; Bozec, H. L.; Rigaut, S. *Chem. Commun.* **2008**, 6117.
(32) (a) Tanaka, Y; Inagaki, A.; Akita, M. *Chem. Commun.* **2007**, 1169. (b) Tanaka, Y.; Ishisaka, T.; Inagaki, A.; Koike, T.; Lapinte, C.; Akita, M. *Chem.-Eur. J.* **2010**, *16*, 4762.
(33) Chan, J. C.-H.; Lam, W. H.; Wong, H.-L.; Zhu, N.; Wong, W.-T.; Yam, V. W.-W. *J. Am. Chem. Soc.* **2011**, *133*, 12690.
(34) Morimoto, M.; Miyasaka, H.; Yamashita, M.; Irie, M. *J. Am. Chem. Soc.* **2009**, *131*, 9823.
(35) Ordronneau, L.; Nitadori, H.; Ledoux, I.; Singh, A.; Williams, J. A. G.; Akita, M.; Guerchais, V.; Bozec, H. L. *Inorg. Chem.* **2012**, *51*, 5627.
(36) He, B.; Wenger, O. S. *Inorg. Chem.* **2012**, *51*, 4335.
(37) Zhong, Y.-W.; Vila, N.; Henderson, J. C.; Flores-Torres, S.; Abruna, H. D. *Inorg. Chem.* **2007**, *46*, 10470.
(38) (a) Jukes, R. T. F.; Adamo, V.; Hartl, F.; Belser, P.; De Cola, L. *Inorg. Chem.* **2004**, *43*, 2779. (b) Fraysse, S.; Coudret, C.; Launay, J.-P. *Eur. J. Inorg. Chem.* **2000**, 1581.
(39) (a) Neilson, B. M.; Lynch, V. M.; Bielawski, C. W. *Angew. Chem., Int. Ed.* **2011**, *50*, 10322. (b) Neilson, B. M.; Bielawski, C. W. *J. Am. Chem. Soc.* **2012**, *134*, 12693.
(40) (a) Lin, Y.; Yin, J.; Yuan, J.; Hu, M.; Li, Z.; Yu, G.-A.; Liu, S. H. *Organometallics* **2010**, *29*, 2808. (b) Lin, Y.; Yuan, J.; Hu, M.; Cheng, J.; Yin, J.; Jin, S.; Liu, S. H. *Organometallics* **2009**, *28*, 6402.
(41) Roberts, M. N.; Nagle, J. K.; Finden, J. G.; Branda, N. R.; Wolf, M. O. *Inorg. Chem.* **2009**, *48*, 19.
(42) Green, K. A.; Cifuentes, M. P.; Corkery, T. C.; Samoc, M.; Humphrey, M. G. *Angew. Chem., Int. Ed.* **2009**, *48*, 7867.
(43) (a) Lebreton, C.; Touchard, D.; Pichon, L. L.; Daridor, A.; Toupet, L.; Dixneuf, P. H. *Inorg. Chim. Acta* **1998**, *272*, 188. (b) Xu, G.-L.; DeRosa, M. C.; Crutchley, R. J.; Ren, T. *J. Am. Chem. Soc.* **2004**, *126*, 3728. (c) Zhu, Y.; Clot, O.; Wolf, M. O.; Yap, G. P. A. *J. Am. Chem. Soc.* **1998**, *120*, 1812. (d) Jones, N. D.; Wolf, M. O.; Giaquinta, D. M. *Organometallics* **1997**, *16*, 1352.
(44) (a) Diez, A.; Lalinde, E.; Moreno, M. T.; Sanchez, S. *Dalton Trans.* **2009**, 3434. (b) Vives, G.; Carella, A.; Sistach, S.; Launay, J.-P.; Rapenne, G. *New J. Chem.* **2006**, *30*, 1429.
(45) (a) Wei, Q.-H.; Yin, G.-Q.; Zhang, L.-Y.; Chen, Z.-N. *Organometallics* **2006**, *25*, 4941. (b) Wei, Q.-H.; Zhang, L.-Y.; Shi, L.-X.; Chen, Z.-N. *Inorg. Chem. Commun.* **2004**, *7*, 286.
(46) (a) Richardson, D. E.; Taube, H. *Inorg. Chem.* **1981**, *20*, 1278. (b) Wenger, O. S. *Chem. Soc. Rev.* **2012**, *41*, 3772. (c) He, B.; Wenger, O. S. *J. Am. Chem. Soc.* **2011**, *133*, 17027. (d) Reuter, L. G.; Bonn, A. G.; Stuckl, A. C.; He, B.; Pati, P. B.; Zade, S. S.; Wenger, O. S. *J. Phys. Chem. A* **2012**, *116*, 7345.
(47) (a) Vacher, A.; Barriere, F.; Roisnel, T.; Piekara-Sady, L.; Lorcy, D. *Organometallics* **2011**, *30*, 3570. (b) Onitsuka, K.; Ohara, N.; Takei, F.; Takahashi, S. *Dalton Trans.* **2006**, 3693. (c) Pu, S.; Fan, C.; Miao, W.; Liu, G. *Dyes Pigm.* **2010**, *84*, 25.
(48) Irie, M.; Lifka, T.; Kobatake, S.; Kato, N. *J. Am. Chem. Soc.* **2000**, *122*, 4871.
(49) (a) Becke, A. D. *J. Chem. Phys.* **1993**, *98*, 5648. (b) Perdew, J. P.; Burke, K.; Ernzerhof, M. *Phys. Rev. Lett.* **1996**, *77*, 3865.
(50) (a) Bauernschmitt, R.; Ahlrichs, R. *Chem. Phys. Lett.* **1996**, *256*, 454. (b) Casida, M. E.; Jamorski, C.; Casida, K. C.; Salahub, D. R. *J. Chem. Phys.* **1998**, *108*, 4439. (c) Stratmann, R. E.; Scuseria, G. E.; Frisch, M. J. *J. Chem. Phys.* **1998**, *109*, 8218.
(51) (a) Cossi, M.; Scalmani, G.; Rega, N.; Barone, V. *J. Chem. Phys.* **2002**, *117*, 43. (b) Barone, V.; Cossi, M.; Tomasi, J. *J. Chem. Phys.* **1997**, *107*, 3210.
(52) (a) Andrae, D.; Haussermann, U.; Dolg, M.; Stoll, H.; Preuss, H. *Theor. Chim. Acta* **1990**, *77*, 123. (b) Schwerdtfeger, P.; Dolg, M.; Schwarz, W. H. E.; Bowmaker, G. A.; Boyd, P. D. W. *J. Chem. Phys.* **1989**, *91*, 1762. (c) Dolg, M.; Wedig, U.; Stoll, H.; Preuss, H. *J. Chem. Phys.* **1987**, *86*, 866.
(53) (a) Pyykkö, P.; Mendizabal, F. *Inorg. Chem.* **1998**, *37*, 3018. (b) Ehlers, A. W.; Böhme, M.; Dapprich, S.; Gobbi, A.; Höllwarth, A.;

Jonas, V.; Köhler, K. F.; Stegmann, R.; Veldkamp, A.; Frenking, G. *Chem. Phys. Lett.* **1993**, *208*, 111.

(54) Frisch, M. J.; Trucks, G. W.; Schlegel, H. B.; Scuseria, G. E.; Robb, M. A.; Cheeseman, J. R.; Montgomery, J. A., Jr.; Vreven, T.; Kudin, K. N.; Burant, J. C.; Millam, J. M.; Iyengar, S. S.; Tomasi, J.; Barone, V.; Mennucci, B.; Cossi, M.; Scalmani, G.; Rega, N.; Petersson, G. A.; Nakatsuji, H.; Hada, M.; Ehara, M.; Toyota, K.; Fukuda, R.; Hasegawa, J.; Ishida, M.; Nakajima, T.; Honda, Y.; Kitao, O.; Nakai, H.; Klene, M.; Li, X.; Knox, J. E.; Hratchian, H. P.; Cross, J. B.; Bakken, V.; Adamo, C.; Jaramillo, J.; Gomperts, R.; Stratmann, R. E.; Yazyev, O.; Austin, A. J.; Cammi, R.; Pomelli, C.; Ochterski, J. W.; Ayala, P. Y.; Morokuma, K.; Voth, G. A.; Salvador, P.; Dannenberg, J. J.; Zakrzewski, V. G.; Dapprich, S.; Daniels, A. D.; Strain, M. C.; Farkas, O.; Malick, D. K.; Rabuck, A. D.; Raghavachari, K.; Foresman, J. B.; Ortiz, J. V.; Cui, Q.; Baboul, A. G.; Clifford, S.; Cioslowski, J.; Stefanov, B. B.; Liu, G.; Liashenko, A.; Piskorz, P.; Komaromi, I.; Martin, R. L.; Fox, D. J.; Keith, T.; Al-Laham, M. A.; Peng, C. Y.; Nanayakkara, A.; Challacombe, M.; Gill, P. M. W.; Johnson, B.; Chen, W.; Wong, M. W.; Gonzalez, C.; Pople, J. A. *Gaussian 03*, revision D.02; Gaussian, Inc.: Wallingford, CT, 2004.